2nd IFAC Workshop on Automatic Control in Offshore Oil and Gas Production,
May 27-29, 2015, Florianópolis, Brazil

Virtual Flow Metering using B-spline Surrogate Models

Bjarne Grimstad * **Patrick M. Robertson** * **Bjarne Foss** *

* *Department for Engineering Cybernetics, NTNU. E-mail: bjarne.grimstad@ntnu.no, patrickm.robertson@gmail.com, bjarne.foss@ntnu.no.*

Abstract: Existing optimization-based virtual flow metering solutions use advanced, black-box process models directly in the optimization problem. This approach has many potential disadvantages, for example: non-smooth models and lack of derivative information may hamper the optimization solver. In this paper a new approach to optimization-based virtual flow metering using B-spline surrogate models is presented. In this approach the black-box process models are replaced with smooth B-spline approximations, with gradients readily available to the solver. We show that the approximation can be done without any significant loss of accuracy. By using surrogate models the optimization solver can be decoupled from the process simulator, saving I/O-operations and evaluations of the process model, resulting in reduced solution times. Another beneficial feature of the problem formulation is that poorly calibrated models may be identified and weighed less in the optimization problem. Some insight on how to select measurement noise and model error weights is shared with the reader.

Keywords: State estimation, data reconciliation, splines, nonlinear programming, modelling errors.

1. INTRODUCTION

Model-based technologies are increasingly used to improve the operability and safety of subsea oil and gas production systems; several testimonials to this can be found in the literature, cf. (Stenhouse, 2008; Foss, 2012). By coupling sensor data with process models, operators may estimate the unknown flow rates in the system. This may aid them in: operating within safety and flow assurance limits, preventing unnecessary wear and tear on the equipment, identifying equipment failure, and in guiding the system to desired operating points.

In modern field developments, accurate pressure and temperature sensors are installed throughout the production system, from the bottom-hole of the wells to the separator. Flow meters are installed more sparingly due to high costs. For additional accuracy and redundancy, the systems are monitored with software that infer the flow rates by inserting available measurements into an advanced process model/simulator. This technology is known as *flow estimation*, *data reconciliation* or *virtual flow metering* (VFM). A survey and discussion on the use of flow estimation in subsea oil and gas production systems can be found in the recent work of Robertson (2014). The same work provides a list of existing commercial and in-house VFM solutions. One example from this list is FMC Technologies' FlowManager$^{\text{TM}}$(Holmås et al., 2011).

A VFM system is an *online* system, running at real-time speed in intervals of seconds or minutes. For this reason, steady-state models have been prevalent in VFM systems to obtain the required solution times. Once within each interval a steady-state flow estimation problem, or data reconciliation problem, is solved to obtain the estimated rates. For a linear process model, this problem is a special case of the Kalman filter (Narasimhan and Jordache, 1999). This relation becomes less clear when a nonlinear model is used and operational constraints are included. The resulting optimization problem is then non-convex and difficult to solve. The situation is not improved by the fact that the process model is considered to be a black-box model without available gradient information. To resolve some of these issues we will in this work replace the process models with B-spline surrogate models. These surrogate models are accurate, smooth, fast to evaluate, and they offer gradients – all being favourable properties for optimization.

Using the B-spline surrogate models, we form a data reconciliation problem that we solve for a semi-realistic case with two subsea wells. A nice feature of the proposed method is that model errors, as well as measurement noise, are considered in the problem formulation. This allows for gross error detection to identify poorly calibrated models, which is a common issue in VFM systems; this is due to the lack of flow rate measurements for model calibration (Bieker et al., 2007).

2. FLOW ESTIMATION

Let $\mathbf{y}$ be an n_y-vector of variables to be reconciled with the corresponding measurements $\bar{\mathbf{y}}$. [1] We denote the difference between the reconciled and measured values with $\mathbf{v}$, i.e. $\mathbf{v} = \mathbf{y} - \bar{\mathbf{y}}$. Furthermore, we denote with an n_x-vector $\mathbf{x}$

[1] Vectors are denoted with bold face $\mathbf{y}$ and vector elements with y_i. All measurements are denoted with a bar accent, e.g. $\bar{\mathbf{y}}$.

the unmeasured variables that we want to estimate. To estimate $\mathbf{x}$ we solve the following nonlinear programming problem

$$\begin{aligned} \underset{\mathbf{x},\mathbf{y},\mathbf{v},\mathbf{w}}{\text{minimize}} \quad & ||\mathbf{v}||^2_{\mathbf{M}} + ||\mathbf{w}||^2_{\mathbf{N}} \\ \text{subject to} \quad & \mathbf{g}(\mathbf{x},\mathbf{y}) = \mathbf{w} \\ & \mathbf{y} - \bar{\mathbf{y}} = \mathbf{v} \\ & \mathbf{x} \in \mathbf{X} \end{aligned} \tag{P}$$

where $\mathbf{g} : \mathbb{R}^{n_x} \times \mathbb{R}^{n_y} \to \mathbb{R}^m$ are m maps between the reconciled (measured) variables y and the unmeasured variables $\mathbf{x}$. In general, $\mathbf{g}$ is a vector of nonlinear functions and, hence, $\mathbf{g}(\cdot) = \mathbf{w}$ describes a nonconvex constraint set. The variables $\mathbf{w} \in \mathbb{R}^m$ represent model errors; in the case of a perfect model $\mathbf{w} = \mathbf{0}$. The set $\mathbf{X}$ is a convex polytope which may include linear constraints on the estimated variables $\mathbf{x}$. Note that the measurements $\bar{\mathbf{y}}$ are not considered variables in $\mathbf{P}$.

The objective of $\mathbf{P}$ is a weighted least-squares quadratic function defined by the norms $||\mathbf{v}||^2_{\mathbf{M}} = \mathbf{v}^\mathsf{T}\mathbf{M}\mathbf{v}$ and $||\mathbf{w}||^2_{\mathbf{N}} = \mathbf{w}^\mathsf{T}\mathbf{N}\mathbf{w}$, representing penalties on measurement and modelling errors, respectively. The matrices $\mathbf{M}$ and $\mathbf{N}$ can be thought of as the inverse covariance matrices for the measurement noise and model errors. In this work we set $\mathbf{M} = \text{diag}(\boldsymbol{\mu})$ and $\mathbf{N} = \text{diag}(\boldsymbol{\nu})$, where $\boldsymbol{\mu}$ and $\boldsymbol{\nu}$ are two vectors of non-negative weights, to obtain diagonal, positive definite matrices and a convex objective function.

Problem $\mathbf{P}$ is a steady-state data reconciliation problem. Next we describe how $\mathbf{P}$ may be configured to estimate the flow rates in a simple subsea production system with two wells. The sequential solution of this problem, incorporating new measurements as they become available, is often termed *virtual flow metering*.

2.1 Formulating a simple flow estimation problem

Here we present a configuration of $\mathbf{P}$ which can be applied to any two-well subsea template tied back through a single pipeline (see Fig. 1). Extensions to include more wells and/or more complex topologies are straightforward.

For a subsea production system the vector of measured variables is typically $\mathbf{y} = [\mathbf{p}^\mathsf{T}, \mathbf{t}^\mathsf{T}, \mathbf{u}^\mathsf{T}]^\mathsf{T}$, with measurements $\bar{\mathbf{y}} = [\bar{\mathbf{p}}^\mathsf{T}, \bar{\mathbf{t}}^\mathsf{T}, \bar{\mathbf{u}}^\mathsf{T}]^\mathsf{T}$, where $\mathbf{p}$ denotes pressures, $\mathbf{t}$ denotes temperatures, and $\mathbf{u}$ denotes choke openings. The unmeasured variables to be estimated are typically the flow rates, i.e. $\mathbf{x} = \mathbf{q}$, where $\mathbf{q}$ denotes the flow rates. The vector $\mathbf{g}$ may include pressure and temperature drop functions, as well as other relations between the variables. Below, we consider some commonly used pressure drop functions. For simplicity we assume perfect temperature and choke opening measurements and fix $\mathbf{t} = \bar{\mathbf{t}}$ and $\mathbf{u} = \bar{\mathbf{u}}$ in the formulation.

The *well performance* is usually described by the *inflow performance relationship* (IPR) which describes the inflow from the reservoir to the wellbore. The IPR depends on factors such as rock properties (e.g. permeability), fluid properties, the well completion, *et cetera*, and relates the liquid rate q_i^{liq} to the flowing bottom hole pressure p_i^{bh}:

$$w_i^{\mathsf{ipr}} = g_i^{\mathsf{ipr}}(p_i^{\mathsf{bh}}, q_i^{\mathsf{liq}}) = p_i^{\mathsf{bh}} - f_i^{\mathsf{ipr}}(q_i^{\mathsf{liq}}), \quad \forall\, i \in \{A, B\}. \tag{1}$$

The *vertical lift performance* (VLP) curve describes the relationship between the well flow and the pressure loss

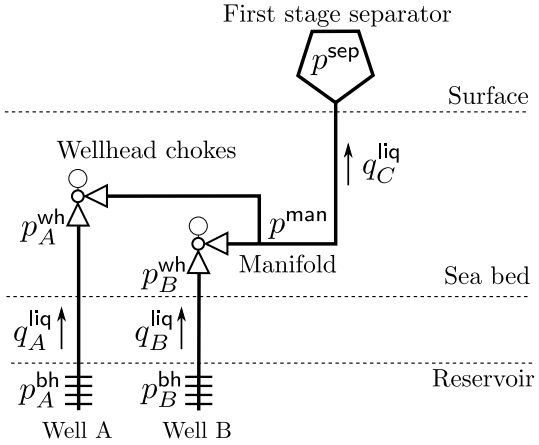

Fig. 1. Topology of production system.

from the bottom hole to the wellhead, and depends on e.g. the well geometry and fluid properties. While a well can be modelled from the reservoir to the wellhead using the IPR and VLP curve, the two models can be combined to create a single *well performance curve* (WPC)

$$w_i^{\mathsf{wpc}} = p_i^{\mathsf{wh}} - f_i^{\mathsf{wpc}}(q_i^{\mathsf{liq}}), \quad \forall\, i \in \{A, B\}. \tag{2}$$

The VLP curve may be ambiguous with respect to flow rate due to gas lifting at low flow rates, therefore we prefer to use the WPC, which is usually more well-behaved.

Wellhead choke valves control the flow rates from each well. The flow rates through the choke valves depend on e.g. choke geometry and the upstream flow regime.

$$w_i^{\mathsf{chk}} = p^{\mathsf{man}} - f_i^{\mathsf{chk}}(q_i^{\mathsf{liq}}, p_i^{\mathsf{wh}}; \bar{t}_i^{\mathsf{wh}}, \bar{u}_i), \quad \forall\, i \in \{A, B\}. \tag{3}$$

The wellhead choke model used in this paper is a multiplier model, which is based on the simple valve equation together with a Morris multiphase multiplier and Chisholm slip correlation (see e.g. Schüller et al. (2003)).

The *flowline* is modelled using the OLGAS 3P multiphase flow correlation. The input variables to the correlation are upstream (manifold) pressure, liquid flow rate, gas-oil ratio (GOR) and water cut (WCT). The measured upstream temperature is considered a fixed parameter. The output is the downstream (separator) pressure:

$$w^{\mathsf{fl}} = p^{\mathsf{sep}} - f^{\mathsf{fl}}(p^{\mathsf{man}}, q_C^{\mathsf{liq}}, r_C^{\mathsf{gor}}, r_C^{\mathsf{wct}}; \bar{t}^{\mathsf{man}}). \tag{4}$$

For convenience, we collect all the model errors in a vector

$$\mathbf{w} = \left[w_A^{\mathsf{ipr}}, w_B^{\mathsf{ipr}}, w_A^{\mathsf{wpc}}, w_B^{\mathsf{wpc}}, w_A^{\mathsf{chk}}, w_B^{\mathsf{chk}}, w^{\mathsf{fl}}\right]^\top,$$

with corresponding weights $\boldsymbol{\nu}$. Similarly, we collect the measurement/reconciliation errors in a vector

$$\mathbf{v} = \left[v_A^{\mathsf{bh}}, v_B^{\mathsf{bh}}, v_A^{\mathsf{wh}}, v_B^{\mathsf{wh}}, v^{\mathsf{man}}, v^{\mathsf{sep}}\right]^\top,$$

with corresponding weights $\boldsymbol{\mu}$.

In addition to the pressure drop constraint functions in $\mathbf{g}$, we model interrelations between the unmeasured variables $\mathbf{x}$ with the constraint set $\mathbf{X}$. For example, we include mass balance constraints on the rate variables $\mathbf{q}$ in $\mathbf{X}$, e.g.

$$q_C^p = q_A^p + q_B^p, \quad \text{for } p \in \{\mathsf{oil}, \mathsf{gas}, \mathsf{wat}\}.$$

Other linear relations that we include in $\mathbf{X}$ are:

$$q_i^{\mathsf{liq}} = q_i^{\mathsf{oil}} + q_i^{\mathsf{wat}}, \quad q_i^{\mathsf{gas}} = r_i^{\mathsf{gor}} q_i^{\mathsf{oil}}, \quad q_i^{\mathsf{wat}} = r_i^{\mathsf{wct}} q_i^{\mathsf{liq}},$$

for $i = \{A, B\}$, where r_i^{gor} and r_i^{wct} are a constant GOR and WCT, respectively.

3. B-SPLINE SURROGATE MODELS

In practice, the nonlinear maps in $\mathbf{g}$, such as the pressure loss functions in the previous section, are given by some process simulator. Most commercially available process simulators are proprietary code and may be considered as "black-box calculators". A process simulator models the production network with complex, nonlinear functions that may be non-smooth in certain regions. Generally, no derivative information is made available and finite difference methods must be used when optimizing with gradient-based solvers, often resulting in a large number of evaluations. Furthermore, when coupling an optimization solver to a (black-box) process simulator, evaluation may be time consuming for several reasons: 1. the simulator may require convergence of the whole network model at each evaluation (even when perturbing a single component of the network), and 2. the IO-operations to transfer data between the solver and simulator may be time consuming. To solve the above problems we will replace the nonlinear maps $\mathbf{g}$ with B-spline approximations $\boldsymbol{\phi}$. The B-splines in $\boldsymbol{\phi}$ are referred to as B-spline surrogate models.

Note that the pressure drop functions in the previous section are on the form $g_i(\cdot) = y_i - f_i(\cdot) = w_i$. Thus, in the following we will approximate f_i (instead of g_i) by ϕ_i, i.e. $\phi_i \approx f_i$, and $g_i \approx y_i - \phi_i$.

3.1 B-splines

A B-spline is a piecewise polynomial function in the variable x, defined by a degree p, a vector of *knots* $\mathbf{t} \in \mathbb{R}^{n+p+1}$, and a vector of n coefficients $\mathbf{c} \in \mathbb{R}^n$ as follows:

$$\phi(x; p, \mathbf{t}) = \mathbf{c}^\mathsf{T} \mathbf{b}(x; p, \mathbf{t}). \tag{5}$$

$\mathbf{b}(x; p, \mathbf{t}) \in \mathbb{R}^n$ is a vector of n B-spline basis functions. The basis functions are overlapping, degree p, polynomial functions, as depicted in Fig. 2 for $n = 8$ and $p = 3$. The basis functions and their derivatives may be evaluated by the numerically stable and fast, recursive algorithms of De Boor (1972) and Cox (1972).

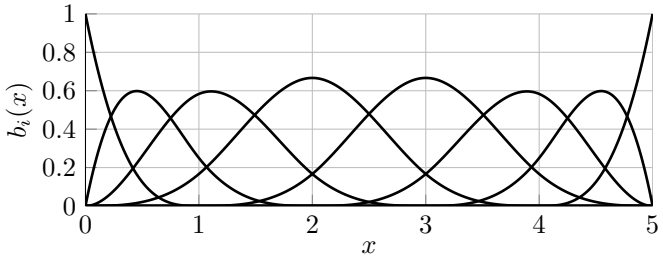

Fig. 2. B-spline basis functions for $p = 3$ and $n = 8$.

The B-spline in (5) generalizes to the multivariate case, where it is called the tensor product B-spline. Most properties of the univariate B-spline, such as a high degree of smoothness and local support, carry over to the multivariate case without any complications. For brevity we will discuss only univariate B-splines in the rest of this section. We note however that the discussion is valid also for tensor product B-splines. The interested reader is referred to the textbooks of Schumaker (1981) and Piegl and Tiller (1997) for an introduction to multivariate splines.

3.2 Cubic spline interpolation

Let any function $f : \mathbb{R} \to \mathbb{R}$, for example f_A^{wpc} in (2), be sampled on a regular (rectangular) grid to yield N data points $\{x_i, f(x_i)\}_{i=1}^N$. Several methods exist for constructing a B-spline that interpolates these N points. These methods vary in how the B-spline degree p and knots $\mathbf{t}$ are selected. The commonly preferred cubic spline ($p = 3$) can be obtain by using a *free end conditions* knot vector

$$\mathbf{t}_F = \{ \underbrace{x_1, \ldots, x_1}_{p+1 \text{ repetitions}}, x_3, \ldots, x_{m-2}, \underbrace{x_m, \ldots, x_m}_{p+1 \text{ repetitions}} \}.$$

To obtain the spline the following linear system is solved for the coefficients $\mathbf{c}$:

$$\underbrace{[\mathbf{b}(x_1)\ \mathbf{b}(x_2)\ \ldots\ \mathbf{b}(x_N)]^\mathsf{T}}_{\mathbf{B}} \mathbf{c} = \mathbf{f}, \tag{6}$$

where $\mathbf{f} = [f(x_i)]_{i=1}^N$ and $\mathbf{B} \in \mathbb{R}^{N \times n}$ is called the B-spline collocation matrix. Note that $\mathbf{b}(x) = \mathbf{b}(x; 3, \mathbf{t}_F)$ in (6).

One advantage with (cubic) spline interpolation is that it avoids the problem of Runge's phenomenon, in which oscillation occurs between the interpolation points (as is evident in interpolation with high degree polynomials). The functions in $\mathbf{g}$ are often polynomial or near-polynomial and approximated by B-splines with little error. The authors' experience with approximating various pressure loss functions suggests that the approximation error typically lies in the order of $0.1 - 0.001\%$ (in fact, the error can be made arbitrarily small by increasing the sampling resolution). Arguably, the error between $\mathbf{g}$ and reality is orders of magnitude larger than this. To illustrate this with an example, let $\phi_N^{\mathsf{wpc}}(q^{\mathsf{liq}})$ be the B-spline approximation of the WPC $f^{\mathsf{wpc}}(q^{\mathsf{liq}})$ sampled in N points. Further, let $e_N(q^{\mathsf{liq}}) = 1 - \phi_N^{\mathsf{wpc}}(q^{\mathsf{liq}})/f^{\mathsf{wpc}}(q^{\mathsf{liq}})$ be the resulting relative approximation error. Approximation errors for $N = 50$, $N = 10$ and $N = 5$ are shown in Figure 3, while error measures are summarized in Table 1.

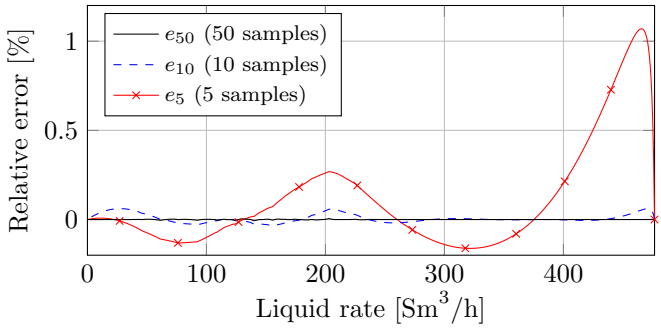

Fig. 3. B-spline approximation errors for a WPC.

Table 1. Maximum errors and 2-norms.

N	$\|e_N\|_\infty$	$\|e_N\|_2$
5	$1.1 \cdot 10^{-2}$	$7.8 \cdot 10^{-2}$
10	$6.1 \cdot 10^{-4}$	$5.7 \cdot 10^{-3}$
50	$6.5 \cdot 10^{-5}$	$2.4 \cdot 10^{-4}$

The construction of a B-spline surrogate model is a two-step procedure: 1. sampling the simulator and 2. solving the linear system in (6) for the B-spline coefficients. This procedure can be run offline and the resulting B-splines stored in advance of optimizing $\mathbf{P}$.

4. RESULTS AND DISCUSSION

4.1 Reference OLGA simulation

To test the performance of the estimator, a production network model representative to Figure 1 was implemented in OLGA, which is considered the *de facto* industry standard for dynamic simulation of multiphase petroleum production systems (Bendiksen et al., 1991; Schlumberger, 2014). A benchmarking simulation was run to obtain a set of noise-free measurements $\{\bar{\mathbf{y}}_k\}_{k=0}^{T}$ (pressures, temperatures and choke positions) and flow rates $\{\bar{\mathbf{q}}_k\}_{k=0}^{T}$, which were assumed to be unknown. Here, k are time indices (the simulation was run for 26 hours with a 10 second sampling interval). In the simulation, the choke valves were sequentially stepped up from 5 % to 60 % opening, as depicted in Figure 4. Default OLGA settings were used.

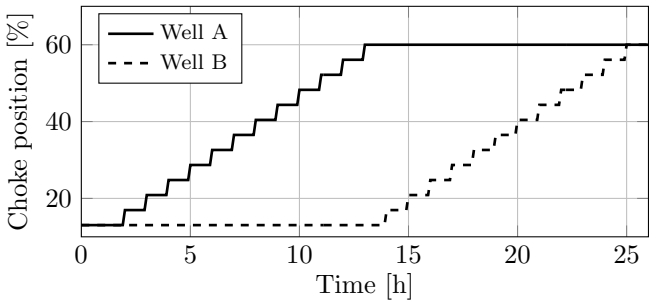

Fig. 4. Choke positions.

4.2 Obtaining the pressure drop models

To equip the estimator with the necessary pressure drop models, a model of the production network was implemented in Petroleum Experts' IPM software package (Petroleum Experts Ltd, 2014). IPRs, WPCs and the flowline model were sampled from the IPM module GAP, and approximated with cubic B-splines. For the chokes, we used a multiplier model based on the valve equation, which was also sampled and approximated with B-splines. Prior to sampling, the models were matched against multi-rate flow tests run in OLGA. The IPRs, WPCs and flowline model were matched using available tools in GAP, while the choke models were matched using a simple multiplication factor. For a large number of samples, it may take a few seconds to generate a B-spline, however, this single calculation is done *offline* and does not contribute to the time taken to solve $\mathbf{P}$.

4.3 Case 1 – Single model evaluation

We first present the estimation results obtained by evaluation each pressure drop model individually. This is equivalent to a nonredundant VFM method which uses a single pressure drop model for estimation. The resulting estimates are presented in Figures 5 (Well A), 6 (Well B) and 7 (Flowline). We note that the IPRs and WPCs tend to underestimate the flow rate slightly, while the choke models tend to overestimate the flow rate. Note how the choke model estimates degrade as the choke opens more, which is due to the increasing sensitivity of the flow rate with respect to pressure as the pressure drop across the choke decreases. The flowline rate estimate displays a large error compared to the well flow rate estimates, indicating that the flowline model is relatively poor.

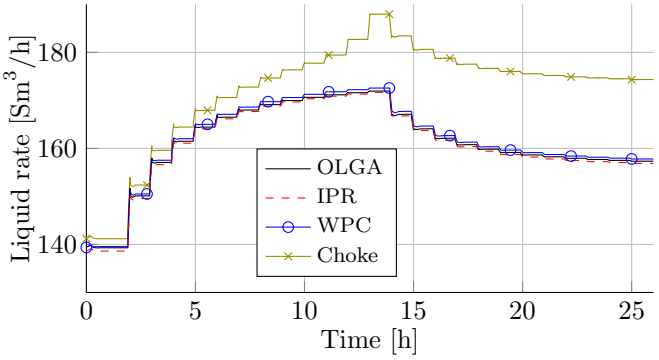

Fig. 5. Estimation by single model evaluation, well A.

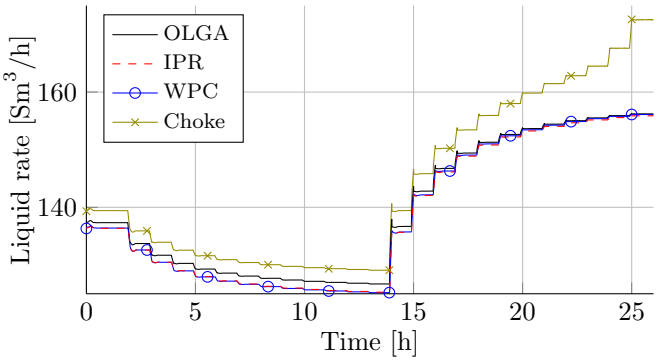

Fig. 6. Estimation by single model evaluation, well B.

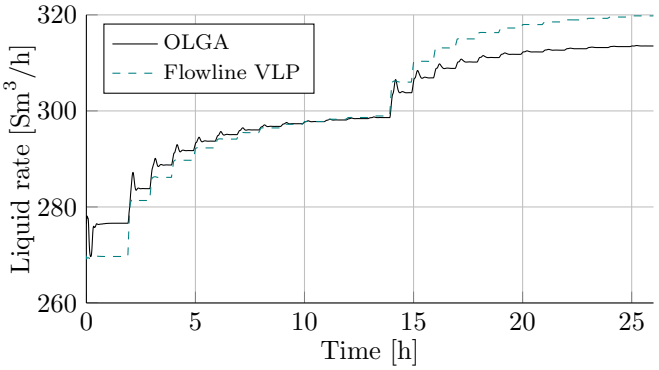

Fig. 7. Estimation by single model evaluation, flowline.

4.4 Case 2 – Uniform weights

Having made a qualitative assessment of the quality of each pressure drop model in Case 1, we now present the estimation results obtained by solving problem $\mathbf{P}$ with uniform weights, i.e. $\mathbf{N} = \mathbf{I}$. Since we have much higher confidence in the pressure measurements than the pressure drop models, $\mathbf{M}$ was configured with relatively large weights; $\mathbf{M} = 10^3 \cdot \mathbf{I}$. For each measurement $\bar{\mathbf{y}}_k$, problem $\mathbf{P}$ was configured as described in Sec. 2.1 and solved to local optimality to obtain the estimate $\mathbf{q}_k$ of the unmeasured flow rates $\bar{\mathbf{q}}_k$.

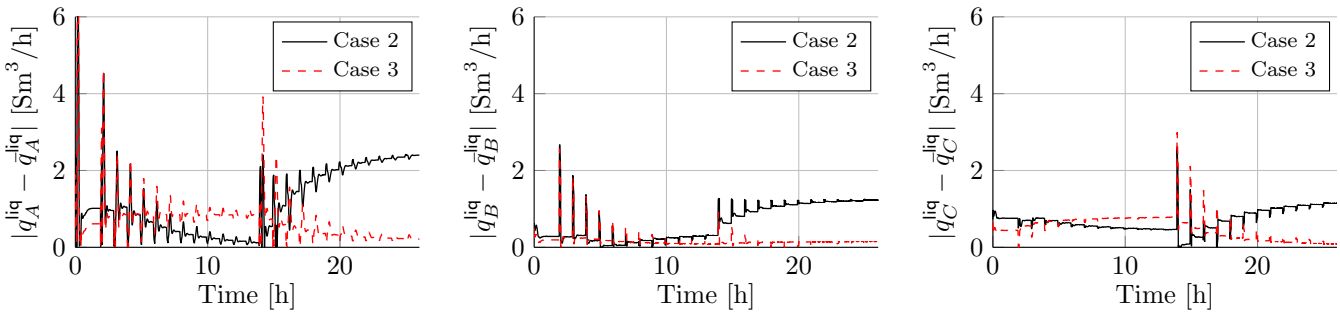

(a) Well A (b) Well B (c) Flowline

Fig. 8. Absolute estimation errors for Case 2 and 3.

Qualitative gross error detection The resulting values of the elements in $\mathbf{w}$ are shown in Figure 9. When qualitatively interpreting this figure, we note that: 1. Small values (i.e. close to zero) indicate that the pressure drop model agrees with the relevant reconciled pressures in the network, and 2. values which are close to each other indicate that the appropriate pressure drop models are in agreement with each other with respect to flow rates. In our case, the model error for the flowline VLP is relatively far from the remaining pressure drop models. This indicates that the rates predicted by the flowline VLP are not consistent with the other pressure drop models (nor with the reconciled pressures), and may be introducing unnecessary estimation errors. This is apparent from Fig. 7, however, in a real-life case, such a figure would not be available. We now proceed to adjusting the model error weights in an attempt to improve the flow rate estimates.

4.5 Case 3 – Heterogeneous weights

Finally, we present the estimation results obtained when we attempt to consider the observations made in Figure 9 and measured model uncertainty through the flow tests. Here, we select the weights $\boldsymbol{\nu}$ based on a normalized sum norm of errors between the measured pressures in the flow tests, and the corresponding pressures predicted by the matched models. The adjusted weights are shown in Table 2. Note the flowline weight ν^{fl} is selected relatively small. Again, we configure and solve $\mathbf{P}$ for each measurement

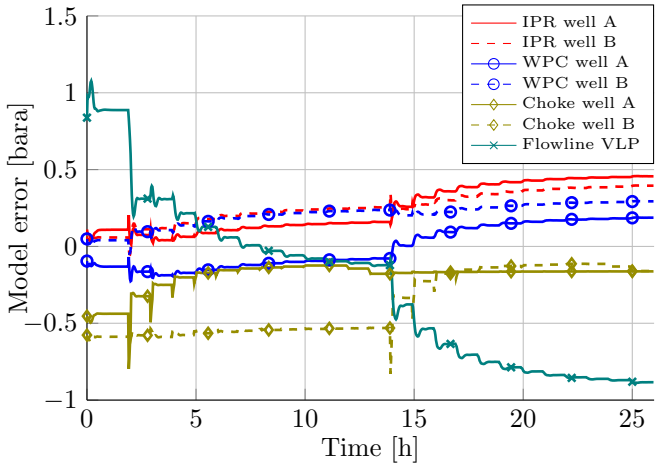

Fig. 9. Model errors with uniform weighting.

$\bar{\mathbf{y}}_k$. The resulting estimation errors in Cases 2 and 3 are shown in Figure 8. A clear reduction in estimation error is seen when our confidence in each model is taken into account through the weighting. In general, as seen in Table 3, the estimates in Case 3 are also better (or near as good) as the estimates produced by any single model. Equally important, we note that using a multi-model formulation increases *robustness* compared to a single-model approach; the resulting estimates become an "agreed consensus" between several models and are less prone to degradation in certain operating conditions (cf. a choke model subjected to a low differential pressure). Note that the spikes in estimation error are caused by unmodelled dynamic behaviour following the choke moves.

4.6 Solution times

The non-convex problems on the form in $\mathbf{P}$ were solved to (local) optimality by the nonlinear programming solver IPOPT (Wächter and Biegler, 2006) on a laptop computer with an Intel Core i7-3740QM CPU running at 2.7 GHz. The solution times are reported in Table 4. We notice that the solution times are below the 10 second real-time limit set by the sampling rate. In fact, as shown by the max-values, all problems were solved well within 10 seconds.

Table 2. Model error weighting $\boldsymbol{\nu}$ in Cases 2/3.

Case	ν_A^{ipr}	ν_B^{ipr}	ν_A^{wpc}	ν_B^{wpc}	ν_A^{chk}	ν_B^{chk}	ν^{fl}
2	1	1	1	1	1	1	1
3	1	0.79	0.25	0.19	0.41	0.37	0.05

Table 3. Mean/max absolute errors (Sm^3/h).

	IPR	WPC	Chk.	FL	Case 2	Case 3
Mean						
Well A	0.42	0.53	10.8	-	0.64	0.17
Well B	0.94	0.88	4.39	-	0.69	0.50
Flowline	-	-	-	3.27	1.20	0.71
Max						
Well A	3.31	2.29	17.0	-	2.67	2.57
Well B	3.87	3.82	16.3	-	2.60	2.99
Flowline	-	-	-	8.81	6.35	7.08

Table 4. Solution times (s).

	IPR	WPC	Chk.	FL	Case 2	Case 3
Mean	0.009	0.010	0.151	0.326	0.496	0.478
Max	0.096	0.093	1.396	2.104	2.472	3.032
% RT*	0.1	0.1	1.5	3.3	5.0	4.8

*Real Time

5. CONCLUDING REMARKS

The proposed method for virtual flow metering was tested on a semi-realistic subsea production system with two wells. The successful test results are encouraging along several axes:

- the process models can be replaced with B-spline surrogate models without any significant loss of accuracy,
- a commercial NLP solver (IPOPT) can efficiently solve a series of data reconciliation problems **P** without any convergence problems (helped by the properties of the B-spline models),
- poorly calibrated models can be identified by analyzing the error variables in the problem formulation.

The authors hope to later improve the proposed method by automating the detection and de-weighting of poorly calibrated models, possibly by including gross error detection in **P**. Several simultaneous procedures for data reconciliation and gross error detection have been presented in the literature (Özyurt and Pike, 2004). These procedures are derived from robust statistics and solve the two problems as one nonlinear program (NLP).

ACKNOWLEDGEMENTS

We acknowledge the support of the Center for Integrated Operations in the Petroleum Industry at NTNU, Norway.

REFERENCES

Bendiksen, K.H., Maines, D., Moe, R., Nuland, S., et al. (1991). The dynamic two-fluid model olga: Theory and application. *SPE production engineering*, 6(02), 171–180.

Bieker, H.P., Slupphaug, O., Johansen, T.A., et al. (2007). Real-time production optimization of oil and gas production systems: A technology survey. *SPE Production & Operations*, 22(04), 382–391.

Cox, M.G. (1972). The numerical evaluation of B-splines. *IMA Journal of Applied Mathematics*, 10(2), 134–149.

De Boor, C. (1972). On calculating with B-splines. *Journal of Approximation Theory*, 6(1), 50–62.

Foss, B. (2012). Process control in conventional oil and gas fields – challenges and opportunities. *Control Engineering Practice*, 20(10), 1058–1064.

Holmås, K., Løvli, A., et al. (2011). Flowmanager^{TM} dynamic: A multiphase flow simulator for online surveillance optimization and prediction of subsea oil and gas production. In *15th International Conference on Multiphase Production Technology*. BHR Group.

Narasimhan, S. and Jordache, C. (1999). *Data reconciliation and gross error detection: An intelligent use of process data*. Gulf Professional Publishing.

Özyurt, D.B. and Pike, R.W. (2004). Theory and practice of simultaneous data reconciliation and gross error detection for chemical processes. *Computers & chemical engineering*, 28(3), 381–402.

Petroleum Experts Ltd (2014). Integrated Production Modelling software (IPM). `http://www.petex.com/products/`. [Online; accessed 29-October-2014].

Piegl, L.A. and Tiller, W. (1997). *The NURBS book*. Springer.

Robertson, P.M. (2014). *Dynamic estimation for controlling a subsea production system*. Master's thesis, NTNU.

Schlumberger (2014). OLGA Dynamic Multiphase Flow Simulator. `http://www.software.slb.com/products/foundation/Pages/olga.aspx`. [Online; accessed 29-October-2014].

Schumaker, L.L. (1981). *Spline functions: basic theory*. Wiley New York.

Schüller, R., Solbakken, T., and Selmer-Olsen, S. (2003). Evaluation of Multiphase Flow Rate Models for Chokes Under Subcritical Oil/Gas/Water Flow Conditions. *SPE Production & Facilities*, 18(3), 170–181.

Stenhouse, B. (2008). Modelling and optimisation in bp exploration and production; case studies and learnings. In *Paper SPE 112148, presented at Intelligent Energy Conference*.

Wächter, A. and Biegler, L.T. (2006). On the implementation of an interior-point filter line-search algorithm for large-scale nonlinear programming. *Mathematical programming*, 106(1), 25–57.